Design and Modeling of a Photonic Crystal Multiplexer Using Artificial Intelligence

Pouya Karami[1], Salah I. Yahya[2,3], Behnam Palash[1], Muhammad Akmal Chaudhary[4], Maher Assaad[4], Fariborz Parandin[1], Saeed Roshani[1], Fawwaz Hazzazi[5], Sobhan Roshani[1,*]

[1]Department of Electrical Engineering, Kermanshah Branch, Islamic Azad University, Kermanshah, Iran
[2]Department of Communication and Computer Engineering, Cihan University-Erbil, Erbil 44001, Iraq;
[3]Department of Software Engineering, Faculty of Engineering, Koya University, Koya KOY45, Iraq
[4]Department of Electrical and Computer Engineering, College of Engineering and Information Technology, Ajman University, Ajman 346, United Arab Emirates
[5]Department of Electrical Engineering, College of Engineering, Prince Sattam bin Abdulaziz University, Al-Kharj 11492, Saudi Arabia

Corresponding author: Sobhan Roshani (sobhan_roshany@yahoo.ca).

ABSTRACT In this paper, design and modeling of an all-optical 2×1 multiplexer based on 2D photonic crystals and artificial neural networks (ANNs) are presented. The proposed structure aims to maximize the difference between the output powers in logical states, which is critical for enhancing the system ability to distinguish between these states. In this study, an ANN model is employed to accurately predict the normalized output power of the designed photonic crystal multiplexer, providing a time-efficient alternative to conventional simulation methods for analyzing multiplexer behavior across various logical states. The results demonstrate significant improvements in signal separation and overall performance compared to previous works. Additionally, a detailed comparison of the normalized output power for different logic states is provided, highlighting the advantages of the proposed design.

INDEX TERMS Photonic crystals, optical multiplexer, all-optical systems, optical communications, silicon photonics, artificial neural networks.

I. INTRODUCTION

IN recent years, the demand for high-speed and high-efficiency processing systems has significantly increased. Traditional electronic systems face limitations, such as low data transfer speeds and considerable energy loss, which are particularly evident in applications involving large data volumes and fast processing [1, 2]. In this context, optical devices have been proposed as a potential solution to overcome these limitations [3, 4]. Optical systems not only reduce energy loss but also enable data transmission at the speed of light without the need for electrical wires [5, 6], leading to a marked improvement in processing performance across various applications.

Two-dimensional photonic crystals are considered one of the key components in the development of fully optical processing systems [7, 8]. Due to their ability to control and guide light at microscopic scales, these structures facilitate the implementation of complex and compact optical circuits [7]. Key applications of photonic crystals include optical filters, sensors, and amplifiers, all of which play a vital role in enhancing the performance of optoelectronic systems [9]. Thanks to their unique properties, photonic crystals have found widespread applications in areas, such as optical communications, optical signal processing, and the design of optical devices [10-12] .

One of the most important components in optical networks and signal processing is the multiplexer. Optical multiplexers allow the combination of multiple input signals into a single output or the separation of a single optical signal into multiple paths [13]. This capability is especially crucial in telecommunications systems, high-speed data transmission, and optical processing [14]. The use of optical multiplexers reduces signal interference, increases bandwidth, and improves data transfer efficiency [15]. Therefore, the design and optimization of these elements are critical for the development of telecommunications systems and optical networks [16].

To enhance the analysis and prediction capabilities of the proposed photonic crystal multiplexer, we incorporate an Artificial Neural Network (ANN) model. ANNs have shown significant potential in different system modeling due to their ability to learn complex, nonlinear relationships and provide accurate predictions in real-time applications [17-19].

In this study, the ANN model is utilized to predict the normalized output power of the multiplexer based on input parameters, such as the logical states, without the need for exhaustive physical simulations. This approach not only reduces computational time but also enables efficient exploration of the multiplexer behavior across different

configurations, contributing to a more flexible and scalable design process for optical devices. Normalized output power refers to the ratio of the actual output power of the multiplexer to its maximum possible output, ensuring a standardized range for easy comparison. Also, logical states represent the binary conditions of the input sources, which determine the multiplexer behavior in controlling optical signal transmission. Moreover, in this study, we aim to minimize the computation time and maximize the difference between output powers in the logical states of 0 (off) and 1 (on). This is an essential feature as it simplifies the distinction between 0 and 1 states, which is the primary advantage of this research over previous works.

II. PROPOSED STRUCTURE FOR A FULLY OPTICAL MULTIPLEXER

To realize a fully optical multiplexer, a square structure of two-dimensional silicon photonic crystals embedded in an air substrate was first used, with eight waveguide paths designed for the inputs and outputs by removing some rods. Table 1 presents the physical specifications of the structure, which consists of a 25×31 grid of two-dimensional photonic crystals. The refractive index of the background is 1, and that of the silicon rods is 3.46, resulting in a refractive index contrast of 2.46, as shown in Fig 1.

TABLE I. Initial Proposed Photonic Crystal Structure Parameters

Parameter	Value	Description
a	0.6 μm	Lattice Constant
R	0.12 μm	Radius of Rods
n1	1	Background Refractive Index
n2	3.46	Rods Refractive Index
-	31×25	Number of Rods

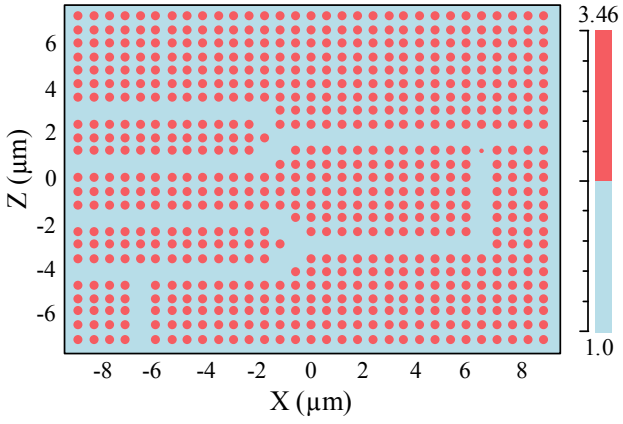

FIGURE 1. Refractive index profile of the presented photonic crystal multiplexer structure.

The photonic bandgap (PBG) of the structure is in the TM mode, as shown in Fig 2, and its range is between 1.42 μm and 2.14 μm. This bandgap range is analyzed using the normalized parameter a/λ, making the results generalizable and comparable. It is expressed as $0.28 < a/\lambda < 0.42$. Therefore, wavelengths shorter than 1.42 μm and longer than 2.14 μm pass through the structure, while wavelengths between these two values do not. Based on these features, the wavelength of the input sources is selected to be 1.55 μm [18, 20]. Due to the periodicity of the photonic crystal structure, a block is considered a unit cell that represents the characteristics of the structure. In the band structure simulation, the unit cell is used to describe the entire structure, and the results obtained are calculated for the periodic arrangement of that cell.

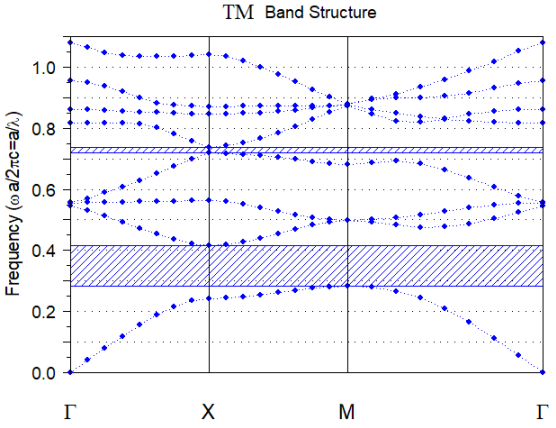

FIGURE 2. Normalized photonic bandgap diagram in TM mode.

In the proposed structure of this study, a defect rod (R1) is used to achieve better results, as shown in Fig 3. The radius of this rod is chosen to be slightly smaller than the other rods, with a value of R1=0.35R, while having the same material as the other rods. The structure includes a bias source at the bottom and two sources for achieving switch S, which can be turned on and off simultaneously, and two other sources for inputs A and B. Based on the location of the sources, the input wave phases are adjusted to obtain the best result.

For this purpose, a phase difference is created between the inputs with its value defined relative to the zero phase. If the phase of input S is considered zero, the other inputs are assigned phase values accordingly, as shown in Figure 3. Input A has a phase of -15°, input B has a phase of -65°, and the bias input has a phase of -55°.

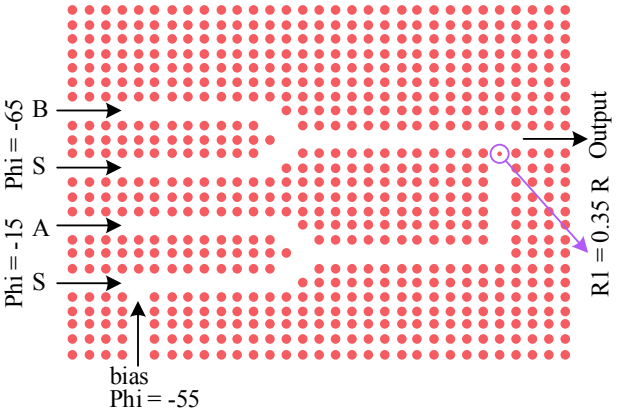

FIGURE 3. Fully optical multiplexer structure proposed in this study.

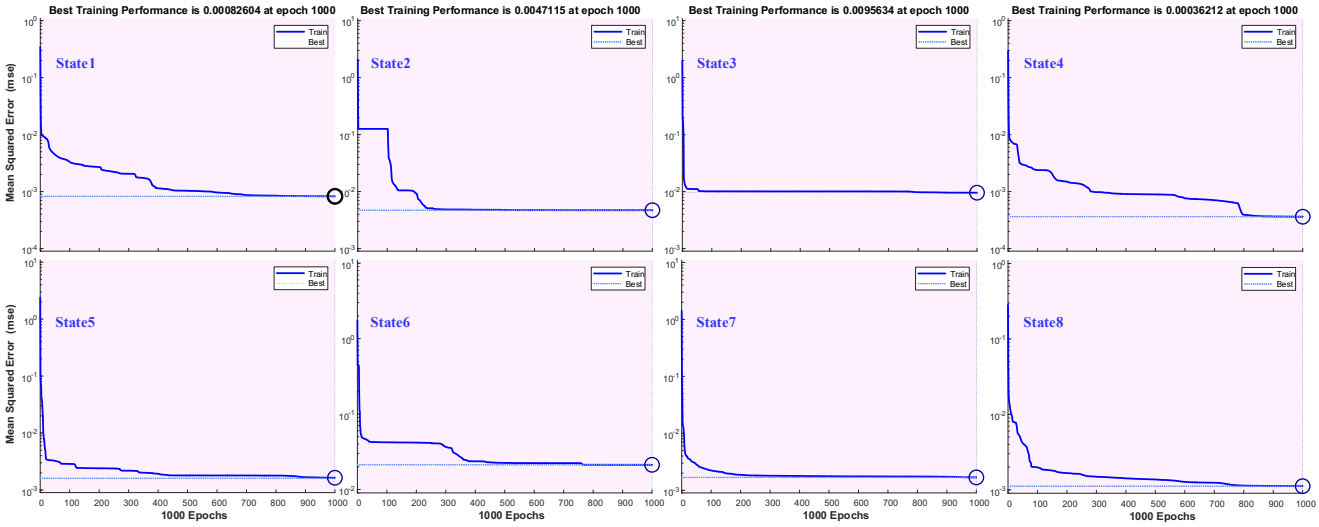

FIGURE 5. Training performance of the proposed ANN model for the designed all-optical multiplexer. In each subplot, the blue line indicates the progression of the training error over 1000 epochs, with the MSE decreasing as the model learns to map inputs to the desired output power. The best training performance for each state is marked with a circle, showing a minimal error value, indicating successful training.

III. ANN MODELING

To enhance the predictive capabilities of our all-optical multiplexer design, we implemented a multilayer perceptron (MLP) neural network. The chosen architecture for the MLP model consists of three layers: two hidden layers with 5 and 7 neurons, and an output layer with 1 neuron. The number of neurons in the first hidden layer is set to 5 neurons for the data with higher nonlinearity and set to 1 neuron for the data with lower nonlinearity for more simplification. The input parameter used in the model is the propagation length, i.e. multiplication of time and light speed (cT), which represents the operational timing associated with the signal transmission in the multiplexer structure. The output of the MLP is the normalized output power, which quantifies the intensity of signal achieved by the multiplexer. While geometric parameters such as the lattice constant, rod radius, refractive index, and defect rod size influence the overall performance of the multiplexer, they were predefined during the simulation phase and not varied within the ANN training process. The presented structure of the MLP model is depicted in Fig. 4 which allows the network to capture the time-dependent behavior of the optical signal, effectively modeling the relationship between timing and output power. By training the network on simulated data, the MLP can predict output power levels across different configurations, facilitating optimization without exhaustive physical simulations.

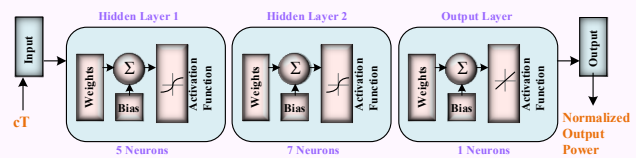

FIGURE 4. The structure of the applied ANN model for the proposed all optical multiplexer.

Figure5 illustrates the training performance of the proposed ANN model across the eight logical states of the all-optical multiplexer. Each subplot represents the training error MSE as a function of epochs for one of the logical states (State 1 to State 8). The training performance converges to its best error value at different rates for each state, demonstrating the ANN model's effectiveness in optimizing for each logical configuration.

Figure 6 illustrates the performance of the applied ANN model in predicting the normalized output power of the proposed all-optical multiplexer in the first logical state of S=0, A=0, and B=0. The close alignment of real and predicted values demonstrates the model accuracy in capturing the multiplexer behavior across various logical states. The results show that the applied ANN model has predicted the multiplexer behavior with high precision, validating the model effectiveness in predicting output power for the multiplexer and providing a time-efficient alternative to traditional simulation methods.

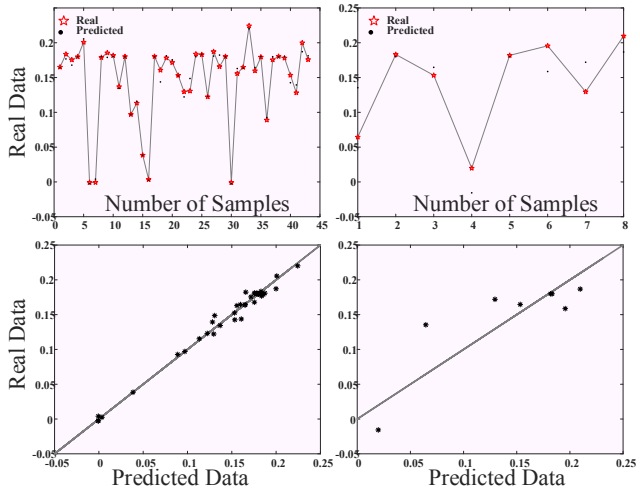

FIGURE 6. Results of the applied ANN model for the proposed all optical multiplexer. The top two plots show a comparison between the real and predicted data across different sample points, with red stars indicating real values and black markers representing predicted data. The bottom two plots provide a scatter plot of real versus predicted data points, allowing further evaluation of the model accuracy. The sampling points in Figure 6 show the training and test data for different normalized output power values as a function of propagation length in the proposed structure. The left scatter plot demonstrates a strong correlation in the training dataset, while the right scatter plot focuses on the test samples, showing some variance but maintaining reasonable accuracy. These variations result from the high nonlinearity in the multiplexer structure; however, they are expected in ANN predictions, and the obtained errors indicate high accuracy.

Table 2 summarizes the performance metrics of the applied ANN model, including Mean Absolute Error (MAE), Root Mean Square Error (RMSE), and Mean Relative Error (MRE) for training and test datasets across various figures. Although there are some variations in the test phase of the proposed ANN model, the MAE, RMSE MRE result highlight the model's accuracy and reliability, with minimal errors observed for most configurations.

TABLE II. Results of the Applied ANN Model

	MAE - Train	MAE - Test	RMSE - Train	RMSE - Test	MRE - Train	MRE Test
State 1	0.0044	0.0282	0.0065	0.0356	0.3169	0.4527
State 2	0.0349	0.0423	0.0673	0.0525	0.1109	1.2479
State 3	0.0136	0.0098	0.0216	0.0125	2.3874	0.0559
State 4	0.0109	0.0386	0.0168	0.0579	0.0649	0.2503
State 5	0.0069	0.0164	0.0104	0.0227	0.0491	6.0935
State 6	5.4e-04	0.0018	0.0010	0.0024	0.0028	0.0089
State 7	0.0234	0.0455	0.0349	0.0629	Inf*	0.1442
State 8	0.0175	0.0423	0.0265	0.0631	0.1912	0.0965

* Infinite (Inf) value of MRE is due to the zero sample in the dataset

IV. RESULTS

The Finite-Difference Time-Domain (FDTD) simulation process is conducted using RSoft FullWAVE. In the designed 2-to-1 multiplexer, there are eight logical states, which are described in the followings. In state 1, all sources are off except for the bias. In state 2, the bias and source A are on, while sources B and S are off, and the output power is 1. In state 3, the bias and source A are off, source B is on, and sources S are off, resulting in zero output. Also, when bias and sources A and B are on, while sources S are off, the multiplexer works in state 4. The bias and sources S are on in states 5, 6, 7, and 8. While, sources A and B are off in state 5, source A is on, and source B is off in state 6, and source B is on and source A is off in state7. Finally, in state 8, all sources in the structure are on.

Figure 7 illustrates the optical power distribution within the proposed multiplexer across all eight logical states. Each subfigure represents a unique state configuration, demonstrating how the input sources (bias, A, B, and S) influence the output power. The distribution patterns highlight the clear differentiation between logical states, with distinct optical intensities for "on" and "off" conditions. This differentiation emphasizes the multiplexer's ability to

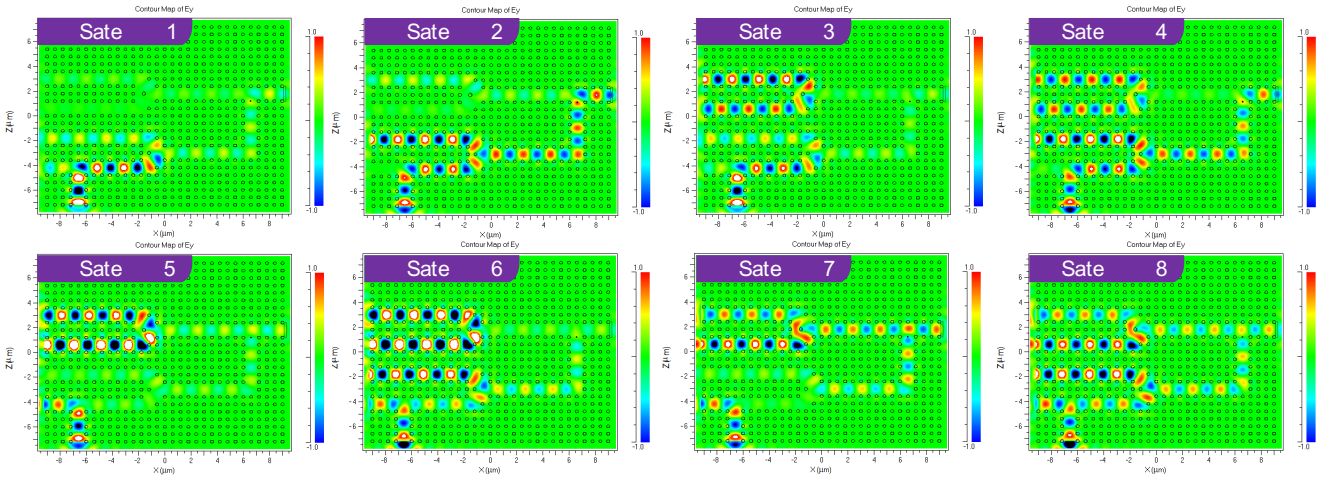

FIGURE 7. Optical power distribution in the proposed 2-to-1 multiplexer across eight logical states. Each state demonstrates distinct output power levels based on the configuration of input sources, validating the multiplexer's capability to differentiate logical states effectively.

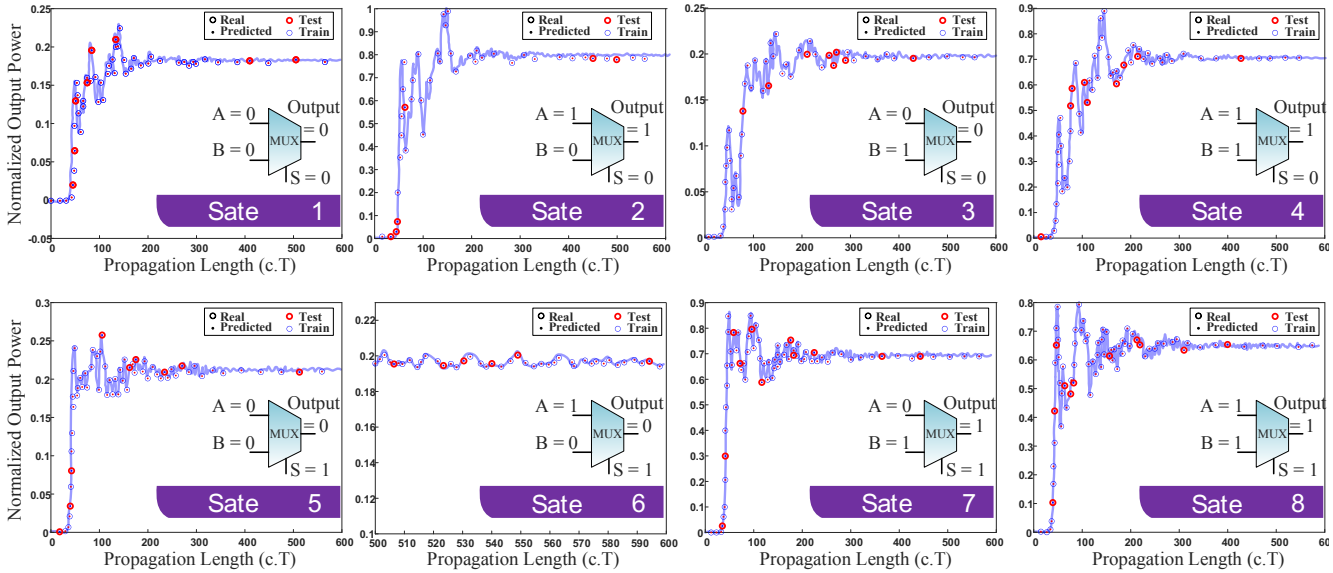

FIGURE 8. Normalized output power distribution of the 2-to-1 multiplexer for eight logical states. Each subplot illustrates the relationship between propagation length and output power, including real, predicted, training, and test data. The annotations clearly indicate the configurations of input sources (A, B, S, and bias) for each state.

effectively separate logical states, ensuring reliable signal processing and improved system performance.

Figure 8 represents the normalized output power of the proposed multiplexer across the eight logical states, with each subplot corresponding to a specific configuration of inputs (A, B, S, and bias). The horizontal axes show the propagation length (c.T), while the vertical axes indicate the normalized output power. The figure demonstrates stable and distinct power levels for "on" and "off" states, ensuring a clear differentiation between logical states. Real, predicted, training, and test data points are also shown in this Figure. The strong alignment between real and predicted data points, as well as minimal discrepancies in training and test data, demonstrates the accuracy and reliability of the ANN model in predicting the proposed multiplexer's behavior.

TABLE III. Comparison of Normalized Output Power for Different Logic States Across Various Studies

Ref	A=B=S=0	A=0 B=1 S=0	A=1 B=0 S=0	A= B=1 S=0	A=B =0 S=1	A=0 B=1 S=1	A=1 B=0 S=1	A= B= S=1
Ideal Values [21]	0	0	1	1	0	1	0	1
[11]	0	0.22	0.53	0.93	0.2	0.67	0.22	0.9
[12]	0.205	0.006	0.555	1.41	0.003	1.77	0.07	2.66
[22]	0	0.15	0.52	0.58	0.08	0.55	0.2	0.57
This work	0.17	0.19	0.8	0.71	0.2	0.72	0.2	0.7

The output results of the proposed multiplexer are compared with results from previous studies, as shown in Table 3. The normalized output power across different logical states demonstrates the significant performance improvements of the proposed design. Specifically, the structure presented in this study achieves better differentiation between logical states, ensuring greater reliability in signal processing and reducing interference. In comparison with prior works, the proposed multiplexer exhibits more consistent and balanced power levels across all states.

Table IV compares the performance of different optical multiplexer designs based on stable time, contrast ratio (CR), maximum and minimum output power (P1min, P0max), computation time, and logical state errors (MSE and RMSE). The MSE and RMSE parameters quantify the deviation between the ideal logical output values and the obtained output values of the multiplexer. The parameters P1min and P0max represent the minimum output power for the expected logical "1" state and the maximum output power for the expected logical "0" state, respectively. The CR (contrast ratio) parameter is defined as the ratio of P1min to P0max. Also, the stable time defines the time which take long for the output power to reach 90% of the stable state. The proposed design achieves the highest contrast ratio (3.5), the lowest stable time (0.3 pS), and significantly reduced computation time (0.64 S vs. >100 S in previous works), which is attributed to the proposed ANN model. Additionally, the lowest MSE (0.05) and RMSE (0.23) indicate improved accuracy in distinguishing logical states. These results confirm that the proposed multiplexer offers better signal separation, faster operation, and higher accuracy, making it more efficient for high-speed optical communication applications.

TABLE IV. Comparison of Performance Metrics for Different Optical Multiplexer Designs.

Ref	Logical States Errors MSE	Logical States Errors RMSE	Time (Sec.)	P1 min	P0 max	CR	Stable Time (ps)
[11]	0.06	0.24	>100 s	0.6	0.25	2.4	0.55
[12]	0.47	0.68	>100 s	0.55	0.2	2.75	0.4
[22]	0.11	0.33	>100 s	0.52	0.2	2.6	0.4
This work	0.05	0.23	0.64 s	0.7	0.2	3.5	0.3

V. CONCLUSION

This research presents the design and modeling of a 2×1 all-optical multiplexer utilizing 2D photonic crystals and artificial neural networks (ANNs). The proposed structure demonstrates a significant improvement in signal clarity and system performance by effectively differentiating between logical states, a critical feature for reliable optical communication. Despite the significant improvements achieved, this study faced several challenges. The trade-off between computational efficiency and prediction accuracy in ANN training required careful tuning to prevent overfitting. Additionally, minor discrepancies in FDTD simulations could affect the ANN model's accuracy. Furthermore, external factors such as temperature variations and nonlinear optical effects were not extensively considered in this design, which may influence practical implementation. The use of photonic crystals enables a compact, energy-efficient, and scalable design, suitable for high-speed optical communication networks and advanced signal processing applications. Additionally, the incorporation of ANNs facilitates accurate performance prediction and optimization, significantly reducing the computational effort compared to conventional simulation methods. Compared to previous works, the proposed multiplexer achieves superior normalized power distribution, reduced signal interference, and enhanced differentiation between logical states.

REFERENCES

[1] R. Soref, "The past, present, and future of silicon photonics," *IEEE Journal of selected topics in quantum electronics,* vol. 12, no. 6, pp. 1678-1687, 2006.

[2] P. Karami *et al.*, "Design of a compact all-optical digital-to-analog converter based on photonic crystals using neural networks," *Results in Optics,* p. 100802, 2025.

[3] B. E. Saleh and M. C. Teich, *Fundamentals of photonics*. john Wiley & sons, 2019.

[4] P. Karami *et al.*, "Design of an optical half-adder based on two-dimensional photonic crystals using feedforward neural networks," *Applied Optics,* vol. 64, no. 4, pp. 973-983, 2025.

[5] Q. Xu, B. Schmidt, S. Pradhan, and M. Lipson, "Micrometre-scale silicon electro-optic modulator," *nature,* vol. 435, no. 7040, pp. 325-327, 2005.

[6] A. A. Mohammed and G. A. QasMarrogy, "Thermal Dynamics in Optical Networks," *ARO-The Scientific Journal of Koya University,* vol. 12, no. 2, pp. 1-9, 2024.

[7] J. D. Joannopoulos, P. R. Villeneuve, and S. Fan, "Photonic crystals: putting a new twist on light," *Nature,* vol. 386, no. 6621, pp. 143-149, 1997.

[8] K. N. Sediq, F. F. Muhammadsharif, S. O. Ramadan, and S. Z. Sedeeq, "Design and study of a nanocavity-based one-dimensional photonic crystal for potential applications in refractive index sensing," *ARO-THE SCIENTIFIC JOURNAL OF KOYA UNIVERSITY,* vol. 11, no. 2, pp. 95-98, 2023.

[9] M. Notomi, "Theory of light propagation in strongly modulated photonic crystals: Refractionlike behavior in the vicinity of the photonic band gap," *Physical Review B,* vol. 62, no. 16, p. 10696, 2000.

[10] E. Yablonovitch, "Inhibited spontaneous emission in solid-state physics and electronics," *Physical review letters,* vol. 58, no. 20, p. 2059, 1987.

[11] F. Parandin and N. Bagheri, "Design of a 2× 1 multiplexer with a ring resonator based on 2D photonic crystals," *Results in Optics,* vol. 11, p. 100375, 2023.

[12] D. G. S. Rao, S. Swarnakar, and S. Kumar, "Design of photonic crystal based compact all-optical 2× 1 multiplexer for optical processing devices," *Microelectronics Journal,* vol. 112, p. 105046, 2021.

[13] V. R. Balaji, M. Murugan, S. Robinson, and R. Nakkeeran, "Design and optimization of photonic crystal based eight channel dense wavelength division multiplexing demultiplexer using conjugate radiant neural network," *Optical and Quantum Electronics,* vol. 49, pp. 1-15, 2017.

[14] D. G. Rabus, "Integrated ring resonators," 2007.

[15] J. K. Poon, J. Scheuer, Y. Xu, and A. Yariv, "Designing coupled-resonator optical waveguide delay lines," *JOSA B,* vol. 21, no. 9, pp. 1665-1673, 2004.

[16] A. Yariv, P. Yeh, and A. Yariv, *Photonics: optical electronics in modern communications*. Oxford university press New York, 2007.

[17] S. Roshani *et al.*, "Mutual coupling reduction in antenna arrays using artificial intelligence approach and inverse neural network surrogates," *Sensors,* vol. 23, no. 16, p. 7089, 2023.

[18] P. Karami *et al.*, "Design of a Photonic Crystal Exclusive-OR Gate Using Recurrent Neural Networks," *Symmetry,* vol. 16, no. 7, p. 820, 2024.

[19] S. Roshani *et al.*, "Design of a Microwave Quadrature Hybrid Coupler with Harmonic Suppression Using Artificial Neural Networks," *Active and Passive Electronic Components,* vol. 2024, no. 1, p. 8722642, 2024.

[20] F. Parandin, P. Karami, and A. Mohamadi, "Machine learning-driven optimization of photonic crystal structures for superior optical NOR gate performance," *Applied Optics,* vol. 63, no. 25, pp. 6666-6673, 2024.

[21] M. M. Mano, *Digital logic and computer design*. Pearson Education India, 2017.

[22] F. Parandin and A. Sheykhian, "Design and simulation of a 2× 1 All-Optical multiplexer based on photonic crystals," *Optics & Laser Technology,* vol. 151, p. 108021, 2022.